www.czasopisma.pan.pl PAN POLSKA AKADEMIA NAUK www.journals.pan.pl

Arch. Metall. Mater. **63** (2018), 4, 2089-2093

DOI: 10.24425/amm.2018.125147

M. MIKUŚKIEWICZ*#, M. STOPYRA*, G. MOSKAL*

SYNTHESIS AND THERMAL PROPERTIES OF EUROPIUM-CERIUM OXIDE AS A NEW FLUORITE-TYPE CERAMIC MATERIAL FOR THERMAL BARRIER COATINGS APPLICATIONS

In the present paper the structure and thermal properties of europium cerium oxides were investigated. The material for the research was obtained via solid state synthesis. The initial powders: ceria CeO_2 and europia Eu_2O_3 were mixed in 1:1 mass ratio (non-stoichiometric proportion with the excess of CeO_2) and milled. The sintering process was performed using high temperature vacuum press at 1350°C. Calorimetric analysis was conducted both for initial powders and milled mixture. The structure, phase composition and thermal diffusivity of obtained material were investigated in as-sintered condition. It was revealed that the obtained material was multi-phase. Non-stoichiometric phases including $Ce_{0.5}Eu_{0.5}O_{1.75}$ with fluorite type structure and different lattice parameters were present. Thermal diffusivity decreased in the range from 25 to 900°C from 1.49 to 0.57 mm^2/s and then increased to 0.70 mm^2/s at 1400°C.

Keywords: TBC, cerium oxide, europium oxide, thermal properties

1. Introduction

The efficiency of aircraft engines strongly depends on the temperature in combusting chamber, therefore in order to limit the fuel consumption and exhaust gases emission the operating parameters of engine need to be increased. With the increase of the working temperature, it is necessary to use more advanced heat-resistant materials. As the operating temperature excess the upper limit of Ni-based superalloys, the ceramic coatings are applied on the crucial engine parts. In the modern aircraft engine turbines thermal barrier coatings (TBC) are commonly used. TBCs in general are double-layer systems, where the outer layer (top-coat) is designed to thermally insulate the base material. The requirements for top-coat material are low heat conductivity, resistance to chemically aggressive environment at high temperature, resistance to thermo-mechanical fatigue and long-term stability of phase composition [1-3]. These coatings are usually plasma-sprayed [4] and the typical material for the top-coat is yttria-stabilized zirconia (8YSZ) [5]. The increasing requirements for the engine operating parameters implies the necessity of developing new materials, with increasingly better insulating properties.

One of the material solution proposed for the new TBC systems are binary oxides with fluorite (F) or pyrochlore (P) type crystal structure and general formula $A_2B_2O_7$ [6], where the A-site is occupied by larger 3^+ cations and the B-site by the smaller 4^+ cations. The difference between pyrochlore and fluorite crystal structure lies in the ordering both in cationic and anionic array, where the oxygen vacancies occur at 8 a site [7]. Thereby, pyrochlore crystal structure can be distinguished from fluorite by the presence of superstructure. The stability of P-type structure is governed by the ratio of cation radii r_A/r_B. It is generally assumed that the systems with $r_A/r_B < 1.48$ exhibit F-type structure, while the values in the range from 1.48 to 1.76 result in P-type structure, wherein ordering of crystal structure depends also on material's thermal history and stoichiometry [7]. The representatives of this group of materials, proposed as top-coat candidates are rare earth metals zirconates [6].

There are plenty of methods for synthesis of rare earth metal pyrochlores and fluorites. They can be generally divided into 2 groups: solid-state-reaction (SSR) and wet-chemistry methods. The input materials in SSR methods are oxide powders, which are mixed in appropriate proportions, homogenized and finally sintered. These methods are relatively simple, but the structure of final product is often inhomogeneous. In the chemical methods (e.g. co-precipitation, sol-gel) the powders are obtained from liquid solutions. Precursors are dissolved and mixed at molecular level which enhances homogeneity [8]. However, the reagents are often more expensive, therefore these methods are preferred when high homogeneity and not necessary large amount of material is needed.

Thermal properties of some of the RE binary oxides with P or F type of structure have been already well characterized in available literature. Among them they are gadolinium [9], neodymium [10], samarium [11] and dysprosium [12] zirconates, mostly obtained via conventional solid state reaction route.

* SILESIAN UNIVERSITY OF TECHNOLOGY, INSTITUTE OF MATERIALSENGINEERING, 8 KRASIŃSKIEGO STR., 40-019 KATOWICE, POLAND

Corresponding author: marta.mikuskiewicz@polsl.pl

However, there are much less information about compounds from europia-ceria (Eu_2O_3-CeO_2) system [13,14]. Ceria is the only one among rare earth oxides which exhibit 4^+ instead of 3^+ oxidation state. Therefore it can occupy B site in $A_2B_2O_7$ compounds. It is also known, that due to ionic radius of Ce4+, no P phase is present in any Ce-RE system. As a large cation, cerium enhances the phonon scattering which contributes to the decrease in thermal conductivity. Hence, it $RE_2Ce_2O_7$ type materials are proposed as good candidates for top-coat materials in TBCs.

In the present paper, the structure and thermal properties of Ce-Eu oxide is investigated. An objective in this paper is to characterize the insulation properties of new materials for TBC applications.

2. Experimental procedure

Nano-crystalline input powders – europium oxide (99.9%, Hefei EV NANO Technology) and cerium oxide (99.9% Hefei EV NANO Technology) were mixed in 1:1 mass ratio (wet-milled in mortar with alcohol). Final product was obtained via solid state reaction in high temperature vacuum press "Degussa" VSPi-15/20 (1350°C/15MPa/2h). Calorimetric studies (DSC 404 F1 Netzsch) were performed for feedstock powders and their mixture after milling. The phase identification of sintered material was carried out using X-ray diffraction (XRD, Jeol JDX-7S diffractometer). The microstructure was investigated using scanning electron microscope (SEM, Hitachi S-3400N) equipped with energy dispersion spectrometer (EDS, Thermo Noran System Six). Thermal diffusivity was measured using Laser-Flash method (LFA 427) in the temperature range 25-1400°C.

3. Results and discussion

Fig. 1 presents results of calorimetric studies. The first peak (at temperature) in the Eu_2O_3 curve is probably related to dehydration. Similar effect was observed in [15]. The peaks at higher temperature are more difficult to interpret. It was reported in [16] that Eu_2O_3 transforms from C (cubic) to B (monoclinic) type at ca. 1100°C which corresponds to location of endothermal peak present designated as "3". Exothermal peaks with maximum at 940°C are present both in CeO_2 and Eu_2O_3 curves. Their interpretation requires further investigation. No peaks are observed during cooling. In the calorimetric curve of Eu_2O_3-CeO_2 mixture first endothermal peak from Eu_2O_3 at 270°C is present. The exothermal peak, which was common to both oxides at 940.9 °C is present. Moreover, no endothermal peak at 1080°C could be observed. These results suggest that formation of new phases preceded by mutual dissolution of constituent oxides took place.

From the results of XRD phase analysis (Fig. 2) it can be concluded that obtained material in as-sintered condition is multi-phase. The most intense peaks were attributed to two types of $Eu_{0.5}Ce_{0.5}O_{1.75}$ phase with fluorite structure (space group $Fm\bar{3}m$) and varying lattice (5.523Å (ICDD card no 04-012-6399) and 5.343Å (ICDD card no 04-006-5865)) parameter. The lattice parameters were read from the ICDD cards and they were not calculated. The small difference in lattice parameters causes broadening of the peaks at lower values of 2Θ, but with the increase in the angle, the peaks become more and more distinctive. The other peaks present in the XRD spectra did not matched any compounds from the Ce-Eu-O system from the database, which suggest the formation of non-stoichiometric phases.

The microstructure of sintered Ce-Eu oxide is presented in Fig. 3. It can be seen from BSE (back-scattered electrons) images that the microstructure is chemically inhomogeneous, as indicated by the noticeable differences in gray level of adjacent areas. The EDS microanalysis was carried out in points marked in Fig. 3b, its qualitative and quantitative results are presented in Fig. 4 and Tab.1. The chemical composition matched phase identified using XRD in areas designated as "2", where ratio of Eu/Ce at.% was close to 1. In the other areas, the Ce/Eu at.% ratio varied from 0.5 to 2.43. The presence of areas characterized by excessive content of both Ce (points 1 and 4) or Eu (point 3) is typical for the materials obtained via conventional solid state synthesis. The formation of new phase takes place on the ceria-europia interface, hence the synthesis process is governed by the diffusion process. Even though feedstock powders were nano-sized, they tend to form conglomerates which hinder the

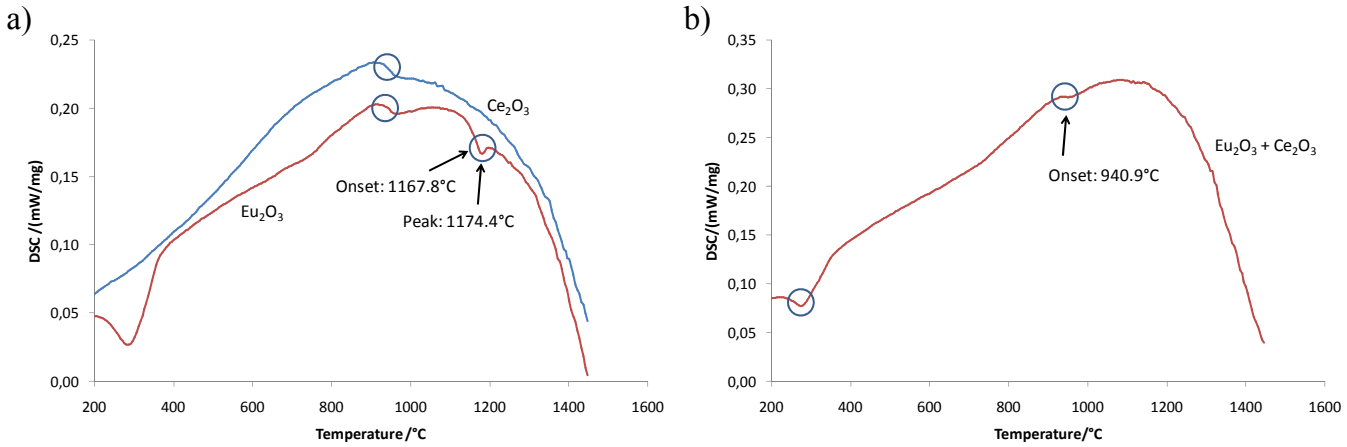

Fig. 1. DSC results for feedstock powders (a) and their mixture (b)

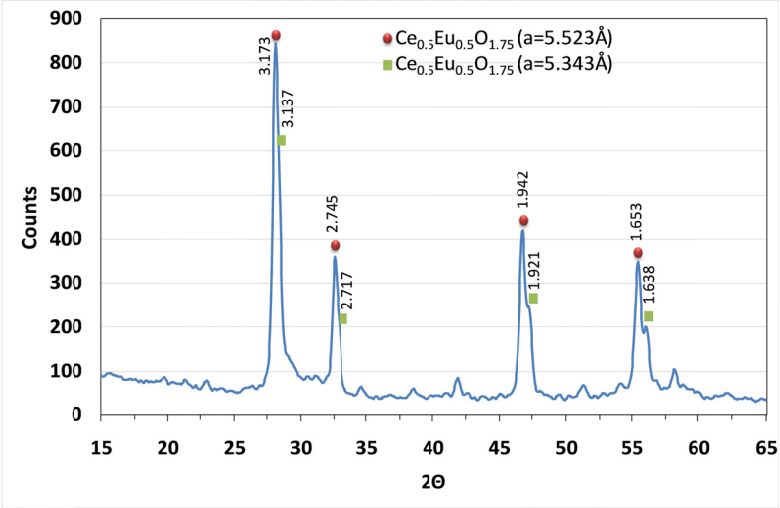

Fig. 2. XRD spectra of sintered Ce-Eu oxide

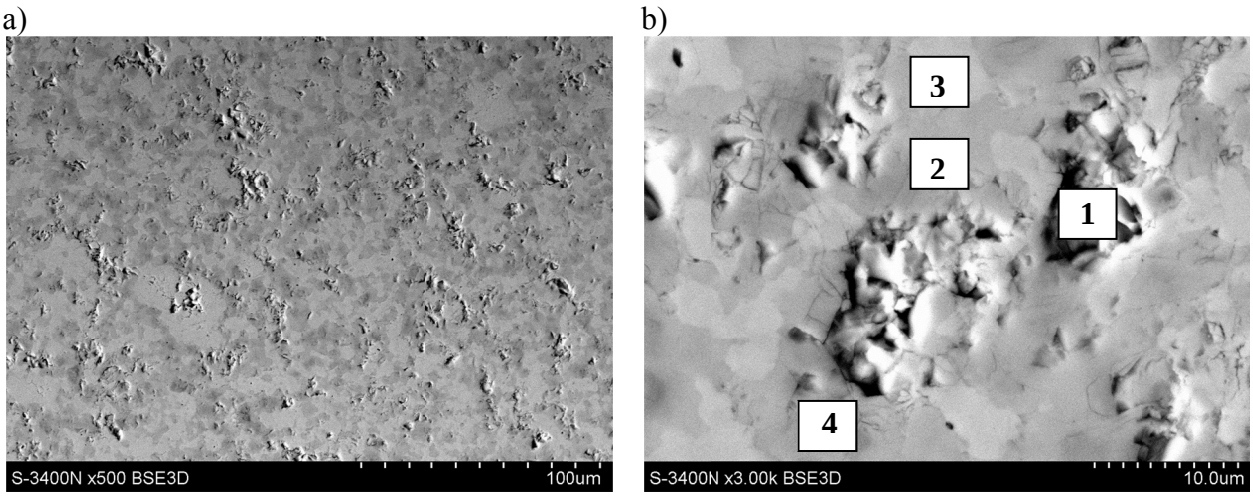

Fig. 3. Microstructure of sintered Ce-Eu oxide (a) and location of spots for EDS analysis (b)

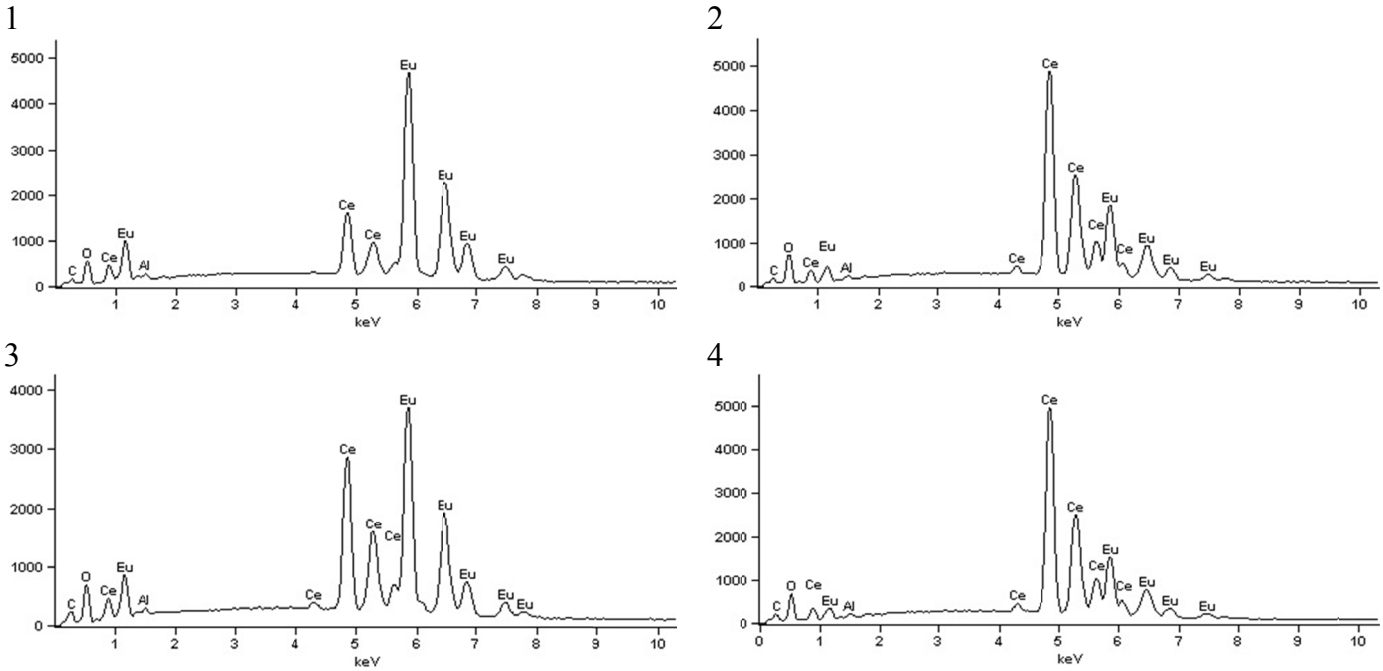

Fig. 4. EDS spectra in accordance to points marked in Fig. 3b

homogenization of mixture. As a consequence, the areas with chemical composition corresponding to $Ce_{0.5}Eu_{0.5}O_{1.75}$ phase (point 2) neighbor areas with varying composition, depending on whether europium oxide was dissolved in cerium oxide or vice versa. This effect can be seen in EDS mapping images (Fig. 5).

TABLE 1

Quantitative results of EDS analysis in points marked in Fig. 3b (at.%)

Point	O	Ce	Eu
1	14.6	50.8	34.6
2	—	50.1	49.9
3	4.6	31.8	63.6
4	3.3	68.7	28.0

Thermal diffusivity of obtained material in temperature range 25-1400°C is presented in Fig. 6. At room temperature thermal diffusivity is 1.49 mm^2/s and it decreases to 0.57 mm^2/s at 900°C. The shape of diffusivity curve suggests that the dominating mechanism controlling the heat transfer in this temperature range is phonon scattering. Comparison between these results and the available literature data concerning $RE_2Ce_2O_7$ leads to the conclusion that thermal diffusivity of investigated Ce-Eu oxide is similar to $Sm_2Ce_2O_7$ obtained with similar method [13]. At temperature higher than 900°C the thermal diffusivity increases and reaches 0.70 mm^2/s at 1400°C, which could be attributed to the increasing share of radiation in overall heat transfer at high temperature.

4. Conclusions

The binary Ce-Eu oxide was synthesized via solid state reaction. The milling in ethanol of constituent oxides did not provide appropriate homogenization of the mixture. As a result, the obtained material exhibited chemical inhomogeneity. Due to the mutual dissolution of cerium and europium oxides, microstructure of sintered material consisted of Ce and Eu-rich areas separated by the areas with intermediate chemical composition and the ratio of Ce/Eu at.% close to 1. The presence of $Ce_{0.5}Eu_{0.5}O_{1.75}$ with fluorite-type structure and varying lattice parameters was revealed. However, considering the chemical composition in micro-areas and results of X-ray diffraction, other non-stoichiometric phases could also be present. Problem of final material`s chemical inhomogeneity and nonstoichiometric phases constituent after synthesis can be solved by multiple

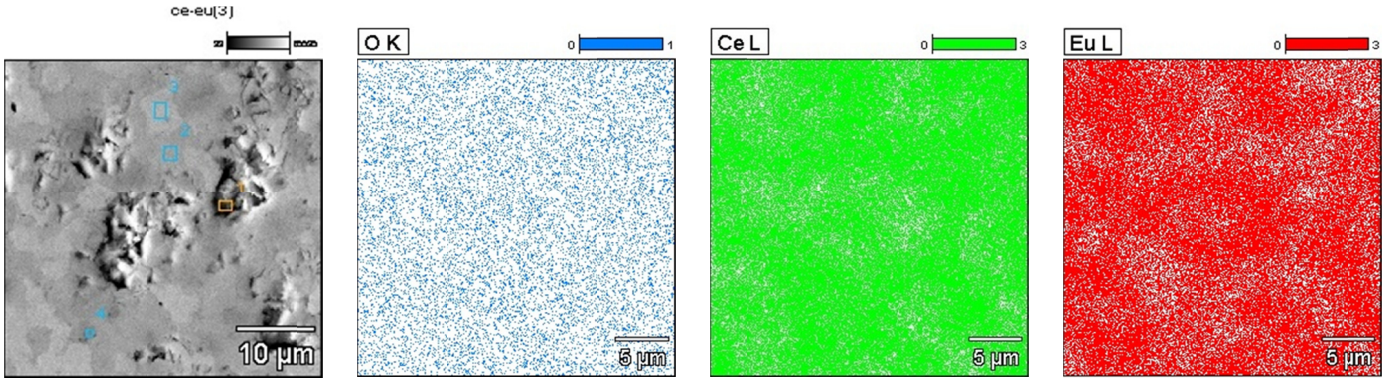

Fig. 5. EDS mapping images for sintered Ce-Eu oxide

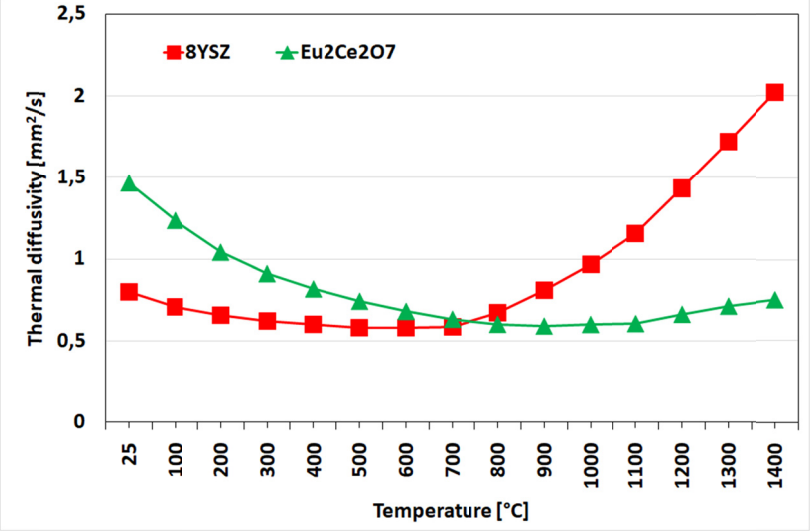

Fig. 6. Thermal diffusivity of sintered Ce-Eu oxide as a function of temperature

milling and re-synthesis in the case of soli state process or by application of co-precipitation method. The thermal conductivity of $Eu_2Ce_2O_7$ is lower than for 8YSZ at temperatures above 700°C due to the stronger radiation effect in 8YSZ. Stronger radiation is a consequence of higher level of porosity or rather total pores boundaries area. The grain boundaries of the pores may emit radiation in this range by means of radiation [17-18]. Thermal diffusivity decreased from 1.49 mm^2 at 25°C to 0.57 mm^2/s at 900°C. Future works will focus on obtaining single-phase binary oxide and further increase in insulating properties.

Acknowledgments

This work was supported by the National Science Centre, Poland under grant number 2016/21/D/ST8/01687.

REFERENCES

[1] A.Y. Zhang, M.K. Lu, G.J. Zhou, S.M. Wang, Y.Y. Zhou, J. Phys. Chem. Solids **67**, 2430-2434 (2006).

[2] M.A. Subramanian, G. Aravamudan, G.V.S. Rao, Prog. Solid State Chem. **15**, 55-143 (1990).

[3] S.V. Ushakov, A. Navrotsky, J. Am. Ceram. Soc. **90**, 1171-1176 (2007).

[4] J.A. Labrincha, J.R. Frade, F.M.B. Marques, Solid State Ionics **99**, 33-40 (1997).

[5] O. Takahisa, I. Katsuhiko, T. Ryoji, O.Y.M. Shinya, Solid State Ionics **167**, 389-387 (2004).

[6] K.E. Sickafus, L. Minervini, R.W. Grimes, J.A. Valdez, M. Ishimaru, F. Li, K.J. McClellan, T. Hartmann, Science **289**, 748-751 (2000).

[7] G. Moskal, L. Swadźba, M. Hetmańczyk, B. Witala, B. Mendala, J. Mendala., P. Sosnowy, J. Eur. Ceram. Soc. **32**, 2025-2034 (2012).

[8] R. Vassen, X.Q. Cao, F. Tietz, D. Basu, D. Stover, J. Am. Ceram. Soc. **83**, 2023-2028 (2000).

[9] X.Q. Cao, R. Vassen, D. Stover, J. Eur. Ceram. Soc. **24**, 1-10 (2004).

[10] M.J. Maloney, Thermal barrier coating systems and materials. U.S. Patent No. 6284323, (2001).

[11] X. Cao, Z. Ma, Y. Liu, Z. Du, K. Zheng, Rare Metal. Mat. Eng. **42**, 1134-1138 (2013).

[12] V.V. Popov, V.F. Petrunin, S.A. Korovin, A.P. Menushenkov, O.V. Kashurnikova, R.V. Chernikov, A.A. Yaroslavtsev, Y.V. Zubavichus, Russ. J. Inorg. Chem. **56**, 1538-1544 (2011).

[13] M. Mikuśkiewicz, G. Moskal, D. Migas, M. Stopyra, Ceram. Int. (2018), DOI: 10.1016/j.ceramint.2018.07.301 (in press).

[14] M.J.D. Rushton, R.W. Grimes, C.R. Stanek, S. Owens, J. Mater. Res. **19**, 1603-1604 (2004).

[15] S. Jucha, G. Moskal, M. Mikuśkiewicz, M. Stopyra, J .Therm. Anal. Calorim. **126**, 1015-1021 (2016).

[16] G. Moskal, M. Mikuśkiewicz, Defect Diffus. Forum **336**, 91-96 (2013).

[17] G. Yang, C. Zhao, Int. J. Heat Mass. Transf. **94**, 199-210 (2016).

[18] B. Wang, C. Zhao, J. Therm. Sci. **111**, 301-309 (2017).